

Two Lyman Continuum Escape Mechanisms at Play in $z \sim 0.3$ galaxies Revealed by Infrared Observations

FANG-TING YUAN,¹ ZHEN-YA ZHENG,¹ CHUNYAN JIANG,¹ AND SHUAI RU ZHU^{1,2}

¹Key Laboratory for Research in Galaxies and Cosmology, Shanghai Astronomical Observatory, Chinese Academy of Sciences, 80 Nandan Road, Shanghai 200030, China

²University of Chinese Academy of Sciences, No. 19A Yuquan Road, Beijing 100049, China

(Received June 1, 2020; Revised March 3, 2026; Accepted March 3, 2026)

Submitted to ApJL

ABSTRACT

We investigate the infrared (IR) properties of a sample of local star-forming galaxies using the WISE data. Focusing on the 20 confirmed strong Lyman continuum (LyC) leakers ($f_{\text{esc}} > 5\%$) included in this sample, we find that the IR detection separates these strong LyC leakers into two populations. The IR-undetected strong leakers in our sample exhibit high $[\text{O III}]5007/[\text{O II}]3725,3727$ (O32) ratios, blue UV slopes, and low stellar masses, consistent with the classical density-bound scenario where the entire ISM is highly ionized. However, IR-bright strong leakers display unexpectedly low O32 ratios while maintaining a substantial escape fraction of $f_{\text{esc}} \sim 12\%$. They also have higher stellar masses and redder UV slopes, similar to weak or non-leakers, along with low nebular extinction, suggesting that the LyC photons are likely to escape through low-column-density channels in a high-density, ionization-bound clumpy medium. Morphologically, these two populations echo the compact starburst and merger-driven LyC leakers observed at $z \sim 3$, indicating that both escape pathways coexist across cosmic time. Our results demonstrate that efficient LyC escape is not limited to the lowest-mass, dust-poor dwarfs but can also occur in more massive, dusty environments, highlighting the potential contribution from dusty systems and posing new questions about the actual dominance of different galaxy populations during the Epoch of Reionization.

Keywords: Starburst galaxies (1570) — Infrared galaxies (790) — Interstellar medium (847) — Reionization (1383)

1. INTRODUCTION

Identifying the physical mechanisms that enable Lyman Continuum (LyC) radiation to escape from galaxies is essential for understanding their contribution to the Epoch of Reionization (EoR). Due to the opacity of the intergalactic medium at $z > 6$, researchers rely on samples at lower redshifts ($z < 4.5$) to identify empirical diagnostics for LyC leakage (e.g., Bergvall et al. 2006; de Barros et al. 2016; Vanzella et al. 2016; Izotov et al. 2016a; Saha et al. 2020; Yuan et al. 2021; Flury et al. 2022a). In particular, local LyC emitters (LCEs or leakers) at $z \sim 0.3$ provide a unique advantage. At

these low redshifts, the impact of IGM absorption is negligible, enabling a robust determination of the absolute LyC escape fraction (f_{esc}).

However, whether these local analogs truly represent the high-redshift population remains unclear. Recent work suggests that high-redshift LyC leakers may be characterized by two distinct physical modes: extreme starbursts and merger-driven systems (Yuan et al. 2024; Zhu et al. 2025; Le Reste et al. 2025). This dichotomy highlights the potential diversity in the interstellar medium (ISM) geometries of leakers, which may not be fully captured by traditional low-redshift selection functions.

Furthermore, although early investigations of LyC escape often include infrared-bright systems such as LIRGs and ULIRGs (e.g., Leitherer et al. 1995; Heckman et al. 2001; Deharveng et al. 2001; Grimes et al.

2009; Cormier et al. 2012), more recent work has shifted toward low-mass, metal-poor, and dust-poor galaxies, which are now commonly used as local analogs of LyC leakers. As a result, the infrared (IR) properties of known LyC leakers have received relatively little attention. In fact, despite low-to-moderate f_{esc} , LyC leakage has been detected in several IR-active galaxies (e.g., Bergvall et al. 2006; Leitet et al. 2013; Borthakur et al. 2014; Roy et al. 2025), indicating that the connection between dust obscuration and LyC escape remains uncertain. Recent studies have highlighted the significance of dust-obscured star formation even at the EoR, suggesting that dust may have accumulated much earlier than previously assumed (e.g., Watson et al. 2015; Laporte et al. 2017; Burgarella et al. 2020; Fudamoto et al. 2021; Álvarez-Márquez et al. 2023; Sun et al. 2025). Given that LyC leakers are expected to be the predominant population during the EoR, we find it imperative to systematically investigate their IR properties to reconcile their dust content with their ionizing escape fractions.

In this work, we use WISE archival data to study a sample of LyC leakers at $z \sim 0.3$. We aim to investigate whether IR observables can provide new insights into the ISM conditions of leakers, particularly in identifying the porous geometries that might allow LyC photons to escape from seemingly dusty or massive systems. We describe the sample and data in Section 2. The main results are presented in Section 3, followed by a discussion of the LyC escape pathways in strong leakers in Section 4. A summary of our findings is provided in Section 5.

2. SAMPLE AND DATA

2.1. Sample of Low-Redshift LCEs

We adopt the galaxy sample from the Low-Redshift Lyman Continuum Survey (LzLCS; Flury et al. 2022a), which consists of 89 star-forming galaxies in the nearby universe ($z \sim 0.3$) observed with the *Hubble Space Telescope* Cosmic Origins Spectrograph (HST/COS). The sample includes 66 new and 23 previously published sources (Izotov et al. 2016a,b, 2018a,b; Wang et al. 2019), resulting in 50 confirmed leakers analyzed uniformly. The sample spans a broad range of physical parameters, including the $[\text{O III}]5007/[\text{O II}]3725,3727$ (hereafter O32) line ratio, UV continuum slope (β_{1200}), stellar mass, star formation rate (SFR), metallicity, and burst age. LyC fluxes and escape fractions (f_{esc}) were measured consistently across the sample.

As in Flury et al. (2022b) and Saldana-Lopez et al. (2022), we define strong leakers as those galaxies with secure LyC detection ($S/N > 5$) and an absolute $f_{\text{esc}} > 0.05$. Weak leakers are sources showing marginal or fair detections ($S/N > 2$) but do not satisfy the strong-leaker

criteria. Non-leakers have no LyC detection ($S/N < 2$). Under such definitions, the sample consists of 20 strong, 30 weak, and 39 non-leakers.

2.2. Infrared Data

We investigate the IR properties of the LzLCS sample using data from WISE (Wright et al. 2010). The angular resolutions of the W1–W4 bands (corresponding to 3.4, 4.6, 12, and 22 μm) are approximately 6.1", 6.4", 6.5", and 12.0", respectively, with 5σ point-source sensitivities in unconfused regions of about 0.08, 0.11, 1, and 6 mJy (Wright et al. 2010; Cutri et al. 2013).

To identify IR counterparts, we cross-matched the sample with AllWISE (Wright et al. 2019) using a 5" radius. After visually inspecting the WISE images to remove cases affected by beam contamination, we classified 37 sources as IR-detected (with $> 2\sigma$ detections in at least one band) and 52 as IR-undetected.

2.3. Emission line data

We measure $[\text{O III}]5007$ and $[\text{O II}]3727, 3729$ fluxes by directly integrating continuum-subtracted SDSS spectra within $\pm 18 \text{ \AA}$ windows. The continuum is estimated from adjacent line-free regions. This approach, which we verified through visual inspection, remains reliable even for asymmetric line profiles. All fluxes are corrected for dust attenuation using $E(B-V)$ provided in Flury et al. (2022a) and the CCM extinction law (Cardelli et al. 1989). Five galaxies with saturated $[\text{O III}]$ lines are excluded, leaving 84 sources for subsequent O32 analysis.

To assess the robustness of our O32 measurements, we compare them with the values reported by Flury et al. (2022a), who use an independent Gaussian-fitting procedure. Despite the methodological differences, 75 out of the 84 galaxies ($\approx 90\%$) agree within 0.2 dex. This high level of consistency demonstrates that our measurements are reliable and broadly consistent with previous work. Moreover, our conclusions remain unchanged when using the Flury et al. (2022a) O32 values.

3. RESULTS

3.1. IR-bright and IR-faint systems

The LyC galaxy sample can be divided into IR-bright (detected) and IR-faint (undetected) systems, summarized in Table 1. The fraction of IR detections in strong, weak, and non-leakers is similar. Within the strong LyC leaker subsample, 8 sources are IR-detected, and 12 are undetected. It is worth noting that all 8 IR-detected strong leakers exhibit significant detections ($> 2\sigma$) in the WISE W3 band, with 5 out of 8 being robustly detected across all four WISE bands. This confirms that our IR-detected strong leaker sample consistently

Table 1. WISE detection statistics of the low- z LCE sample.

Category	All	IR detected	Detection fraction
Strong	20	8	0.4
Weak	30	15	0.5
Non-leaker	39	14	0.36

exhibits detectable mid-IR emission, likely originating from dust components.

We also notice that when dividing the sample into WISE-detected (37 galaxies) and WISE-undetected (52 galaxies), the fraction of strong LyC leakers is remarkably similar (21% vs 23%). Given that they exhibit similar SFRs, the higher IR luminosity reflects a more dust-enriched ISM. The presence of a substantial fraction of leakers in this IR-bright subsample suggests that substantial LyC escape is still possible in a dust-rich environment. This is consistent with previous findings that some IR-bright Lyman Break Analogs may leak a considerable fraction of ionizing radiation (e.g., Heckman et al. 2011; Borthakur et al. 2014), although this interpretation has been questioned in earlier work by Overzier et al. (2009).

The f_{esc} of LyC photons in each subsample is shown in Figure 1 (top). Within the strong leaker population, IR-undetected sources exhibit systematically higher escape fractions than IR-detected ones (median $f_{\text{esc}} = 32.6\%$ vs. 12.4%). Despite this internal difference, IR-detected strong leakers still maintain f_{esc} values significantly exceeding those of the weak leakers, whose f_{esc} remain consistently low (median $\leq 3\%$) regardless of IR detection.

To check for potential f_{esc} overestimation due to IR-omitted SFR measurements, we performed SED fitting with CIGALE (Burgarella et al. 2005; Noll et al. 2009; Boquien et al. 2019) incorporating IR data. The overall impact is limited, with the median f_{esc} of the IR-detected strong leakers shifting to 11.9%.

3.2. Infrared detection versus $O32$

We assess the ISM ionization state using $O32$ for both the IR-detected and IR-undetected systems. Within the strong LyC leakers, the two subsamples exhibit a clear and systematic difference in $O32$. IR-undetected strong leakers preferentially exhibit higher $O32$ values, whereas IR-detected strong leakers occupy a regime of comparatively lower $O32$ (Figure 1, bottom). The median $O32$ of the IR-undetected subsample is higher by $\Delta O32 \approx 9.6$ (Table 2). The permutation test yields a median difference of -9.56 , with a permutation p -value of 0.002, indicating that the observed difference is highly unlikely to arise by chance. A bootstrap analysis gives a consis-

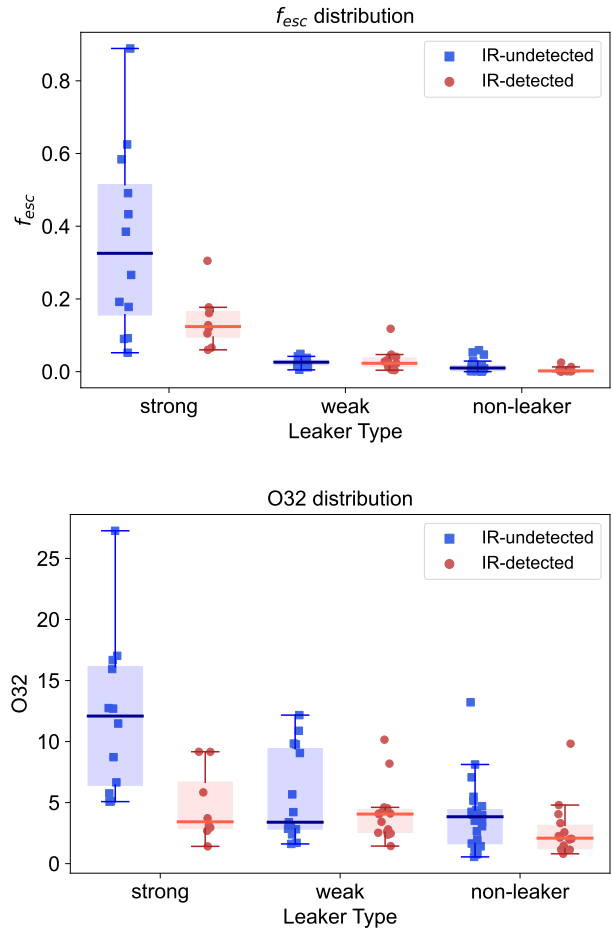


Figure 1. Top: Distribution of f_{esc} for strong, weak, and non-leakers with and without WISE IR detections. Bottom: Distribution of $O32$ for the same categories. In each panel, individual galaxies are shown as jittered blue squares (IR-undetected) and red circles (IR-detected). For each category, the horizontal line denotes the median, and the box contains the middle 50% of the data. The vertical lines extend 1.5 times the height of the box.

tent median difference of -9.70 , with a 95% confidence interval of $[-12.82, -3.82]$. Both tests therefore show that the difference between the two subsamples is statistically significant.

While our sample has been pre-screened via optical spectroscopy to exclude AGN contamination, obscured AGN activity remains possible. Using WISE color-color criteria (Stern et al. 2012), we identify one IR-detected strong leaker, J1442-0209, at the edge of the AGN selection region. This source exhibits the highest $O32$ ratio (~ 9.16) among the IR-detected strong leakers. If we remove this source from our sample, the difference between the two subsamples would be further enhanced.

This systematic difference in the ionizing state between IR-detected and IR-undetected strong leakers may suggest that the two subsamples reflect two distinct LyC-leaking regimes. The IR-undetected strong leakers exhibit globally elevated ionization conditions consistent with a density-bound geometry. On the other hand, the IR-detected strong leakers show modest O32 despite their substantial LyC leakage. This behavior is unexpected, as previous studies consider high O32 to be a necessary or primary indicator of LyC escape (Nakajima et al. 2020; Jaskot et al. 2024). A plausible explanation is that in these IR-detected systems, LyC photons escape through localized, low-density channels rather than through a galaxy-wide density-bound medium. In such a regime, the global O32 ratio does not necessarily reflect the physical conditions along the specific escaping sightlines, allowing for high f_{esc} even at modest overall ionization levels. The systematic difference in O32 provides key evidence that these two subsamples may follow distinct LyC-leaking pathways, a possibility we explore further in Section 4.1.

This distinction can explain why O32 loses its robustness in tracing LyC leakage in some cases, which is not expected in a density-bound scenario. As shown in Figure 2, the detection fraction increases monotonically with O32 for the IR-undetected strong LyC leakers. However, this trend does not hold for the IR-bright strong leakers: their detection rate remains almost flat as the O32 increases.

3.3. Physical properties of the IR-detected and IR-undetected strong LyC leakers

Local strong LyC leakers can be separated into two distinct populations based on their IR emissions. Table 2 summarizes the median values and standard deviations of the physical properties of the IR-detected and IR-undetected subsamples. The IR-undetected strong leakers exhibit the highest f_{esc} , the highest O32, and the bluest β_{1200} among all subsamples. They also have the lowest stellar masses and dust extinction, consistent with a dust-poor, compact, and highly ionized population.

In contrast, while IR-detected strong leakers exhibit significantly higher f_{esc} than weak or non-leakers, their O32 and β_{1200} values are similar to those of the lower-leaking populations. Dust extinction appears to be a key feature distinguishing IR-detected leakers from weak or non-leakers. Despite being IR-luminous, these strong leakers show significantly lower $E(B - V)$ values (derived from SDSS spectra; Flury et al. 2022a) than weak and non-leakers, suggesting a spatial decoupling between their IR and optical emissions. As in the

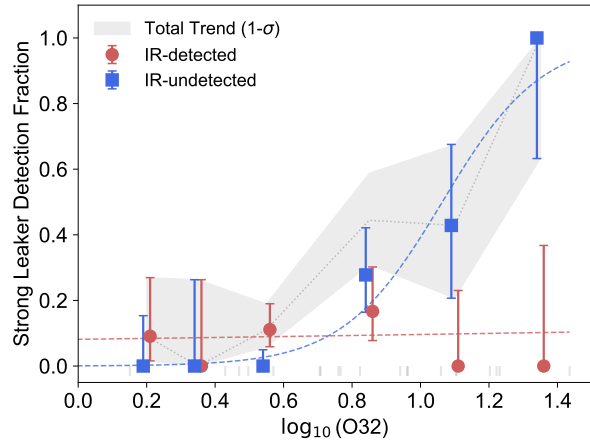


Figure 2. LyC detection fraction as a function of $\log\text{O32}$. The IR-undetected systems (blue squares) show a rising LyC detection fraction with increasing O32 (blue dashed line), consistent with O32 tracing globally high ionization conditions. In contrast, the IR-detected strong leakers (red dots) exhibit an approximately constant detection fraction across the full O32 range (red dashed line), indicating that their LyC escape is not strongly linked to the galaxy-wide O32 ratio. The shaded region indicates the overall detection fraction for the combined sample. At low O32, the total detection fraction is dominated by the IR-detected population, producing a weak trend in the combined sample.

“picket-fence” configuration, the ionizing radiation escapes through low-density channels, avoiding the dense dust clouds that drive the IR luminosity. Conversely, the higher $E(B - V)$ observed in weak and non-leakers indicates an ISM with a higher covering factor, where diffuse dust acts as a continuous screen that both increases optical reddening and suppresses LyC escape. This distinction may also be attributed to orientation effects (Maulick & Saha 2026).

The high stellar mass and red β_{1200} of IR-detected strong leakers seem to deviate from the empirical trends established in previous studies (e.g. Chisholm et al. 2022; Pahl et al. 2023), which associate such properties with lower LyC leakage. Our findings, along with recent reports of massive ($> 10^{10} M_{\odot}$) leakers (Roy et al. 2025; Maulick & Saha 2026), suggest that significant LyC escape remains possible in massive and dusty systems.

4. DISCUSSION

4.1. Two populations of strong LyC leakers?

Our analysis indicates that the IR-detected and IR-undetected strong LyC leakers may be influenced by distinct escape mechanisms. The IR-faint systems appear broadly consistent with a density-bound scenario. In these galaxies, a low neutral hydrogen column density

Table 2. Median physical properties of the IR-detected and IR-undetected subsamples. The number of galaxies in each subsample is given in parentheses.

Property	Strong Leakers		Weak Leakers		Non-leakers	
	IR-non (12)	IR-det (8)	IR-non (15)	IR-det (15)	IR-non (25)	IR-det (14)
f_{esc}	0.33 ± 0.25	0.12 ± 0.07	0.03 ± 0.01	0.02 ± 0.03	0.01 ± 0.02	0.00 ± 0.01
O32	12.70 ± 6.16	3.14 ± 2.40	3.81 ± 3.67	4.06 ± 2.21	3.84 ± 2.72	2.09 ± 2.25
β_{1200}	-2.27 ± 0.97	-1.64 ± 0.99	-1.66 ± 0.39	-1.51 ± 0.63	-1.62 ± 0.78	-1.22 ± 0.96
Age (Myr)	4.69 ± 1.92	5.19 ± 1.36	5.27 ± 1.02	3.44 ± 1.55	5.38 ± 2.05	4.39 ± 1.89
R_{50}	0.38 ± 0.09	0.41 ± 0.08	0.68 ± 0.25	0.56 ± 0.31	0.64 ± 0.45	0.96 ± 0.61
$\log \text{SFR}_{\text{H}\beta} (M_{\odot} \text{ yr}^{-1})$	1.13 ± 0.29	1.40 ± 0.29	0.93 ± 0.34	1.40 ± 0.23	0.91 ± 0.37	1.25 ± 0.20
$\log M_{\star} (M_{\odot})$	8.45 ± 0.50	9.22 ± 0.61	8.73 ± 0.60	8.96 ± 0.75	8.67 ± 0.75	9.59 ± 0.71
$L(22\mu\text{m}) (10^{10} L_{\odot})$	–	4.3 ± 2.3	–	3.7 ± 2.0	–	2.8 ± 1.3
$E(B - V)$	0.05 ± 0.03	0.09 ± 0.05	0.15 ± 0.05	0.17 ± 0.06	0.14 ± 0.12	0.25 ± 0.08
$\log M_{\text{dust}} (M_{\odot})^a$	–	7.22 ± 0.62	–	7.16 ± 1.94	–	7.30 ± 1.42

^a Dust masses are derived using CIGALE SED fitting with the [Draine et al. \(2014\)](#) dust models, based on a subsample of 25 galaxies with IR detections ($> 2\sigma$) in all four WISE bands.

likely allows the ionized region to extend to the galactic boundary. Given a standard dust-to-gas ratio, such systems would naturally be dust-poor, leading to faint, and therefore undetected IR emission.

Conversely, the IR-bright systems could potentially be described by ionization-bound geometries with a porous ISM. In this framework, substantial dust reservoirs ($M_{\text{dust}} \approx 1.7 \times 10^7 M_{\odot}$) could coexist with LyC leakage if the escape is highly anisotropic, occurring through low-column-density channels. While the bulk of ionizing photons is absorbed and reprocessed into IR emission, a significant fraction can still escape through these channels. This would explain why their global observables (like O32 or β_{1200}) appear decoupled from their high f_{esc} . These systems may share the same leakage geometry as the high-redshift sources that exhibit spatially offset LyC emission relative to the rest of the galaxy (e.g., [Yuan et al. 2024](#); [Gupta et al. 2024](#); [Maulick et al. 2025](#); [Ji et al. 2025](#); [Rivera-Thorsen et al. 2025](#)).

The Ly α profile may provide information on the gas density and geometry of a galaxy (e.g., [Schaerer et al. 2011](#); [Verhamme et al. 2015](#); [Hu et al. 2023](#); [Pahl et al. 2024](#)). In our sample, 9 strong leakers were observed with the COS medium-resolution spectrograph (G160M), comprising 2 IR-detected and 7 IR-undetected sources. All 7 IR-undetected galaxies exhibit double-peaked profiles, though the secondary peak in J1121+3806 is relatively faint. It is worth noting that 5 of these sources satisfy the criteria proposed by [Verhamme et al. \(2015\)](#), specifically a small shift of the profile maximum compared to the systemic redshift $v_{\text{peak}} < 150$ km/s and a small peak separation $v_{\text{sep}} < 300$ km/s,

indicating low H I column densities and a high likelihood of LyC leakage. J1233+4959 and J0925+1403 represent borderline cases; while their v_{sep} values (352.8 and 308.5 km s⁻¹) slightly exceed the nominal threshold, they remain largely consistent with the kinematics of leakers. Furthermore, 6 out of 7 IR-undetected sources display a red peak asymmetry $A_r < 3$ (as defined in [Kakiichi & Gronke 2021](#)), suggesting that these systems may be closer to a density-bound regime where LyC photons escape through a globally low H I column density. The only exception is J1243+4646, whose higher asymmetry ($A_r = 4.07$) is likely associated with its complex multi-peaked profile, possibly reflecting a more disturbed gas geometry compared to the rest of the subsample.

Regarding the IR-detected sources, J1152+3400 presents a multi-peaked structure where the two primary peaks fulfill the escape criteria ($v_{\text{peak}} = 147.9$ km/s, $v_{\text{sep}} = 272.2$ km/s). Its high red-peak asymmetry ($A_r = 5.1$) supports a ‘‘picket-fence’’ scenario where leakage occurs through low-density H I holes in a clumpy ISM ([Kakiichi & Gronke 2021](#); [Hu et al. 2023](#)). In contrast, J1333+6246 displays a single dominant peak centered near the systemic redshift ($v_{\text{peak}} = 67.8$ km/s) with a lower $A_r = 1.87$, potentially indicating significant escape through a direct line-of-sight channel ([Verhamme et al. 2015](#); [Hu et al. 2023](#)). These diverse A_r values, combined with the kinematic data, suggest that IR-detected leakers rely on anisotropic channels to facilitate escape from substantial reservoirs, while IR-undetected sources may favor a more uniform, density-bound geometry.

To further characterize the ISM of these strong LyC leakers, we utilize 3 GHz and 6 GHz radio continuum data from the VLA observation presented by [Bait et al. \(2024\)](#). At these frequencies, the radio flux density provides a dust-extinction-free probe of dense star-forming regions, offering an independent diagnostic of the ISM conditions that complements our optical and IR observations. Although this radio analysis is limited to a sub-sample of 6 sources, the results reveal a striking 100% correspondence between IR and radio detections that reinforces our proposed classification. Specifically, the 2 IR-undetected leakers remain undetected in the radio bands, with flux densities falling below the sensitive VLA detection limits. This radio-silent nature provides evidence for a density-bound scenario, where an extremely diffuse and highly ionized ISM lacks the gas density necessary to sustain robust radio emission. In contrast, the 4 IR-bright strong leakers are all robustly detected at both 3 GHz and 6 GHz, confirming the presence of a substantial, high-density ISM. The coexistence of significant LyC escape and strong radio/IR emission in these systems supports an ionization-bound, clumpy medium hypothesis. Despite the small sample size, the alignment between IR and radio properties suggests that these two populations represent physically distinct pathways for photon escape in the local universe.

4.2. Connection between low- z and high- z LyC leakers

The IR-faint and IR-bright systems could potentially align with the starburst- versus merger-driven modes discussed in previous high-redshift ($z > 3$) studies ([Zhu et al. 2025](#)). For instance, while compact starbursts may favor density-bound escape, the gravitational transitions or feedback in more extended, possibly merging systems could naturally create the fragmented ISM structure required for anisotropic leakage. The role of galaxy mergers in facilitating LyC escape remains a subject of active debate (e.g., [Yuan et al. 2024](#); [Le Reste et al. 2025](#); [Maschia et al. 2025](#); [Wang et al. 2025](#)).

We examine high-resolution HST imaging for a subset of our sample (11 of the 20 strong leakers, Figure 3). There are 5 strong leakers with imaging available from the LACOS ([Le Reste, Alexandra 2025](#)) project. Additional 6 strong leakers have been observed by other HST projects¹. Figure 3 shows that the IR-detected leakers exhibit clear merger morphologies, whereas the

IR-undetected leakers appear compact. These imaging results provide preliminary support that IR-bright and IR-faint leakers might correspond to merger-driven and extreme starburst modes, respectively. We note that the wavelength coverage is important for identifying the merging features. As in the galaxy J091703+315221, the secondary is only visible at optical wavelengths (F438W, F547M, and F850LP). Future high-resolution optical images will be necessary to further confirm this conclusion.

5. SUMMARY

We investigate the IR properties of a local sample of 89 star-forming galaxies, including 20 strong LyC leakers. We categorize the sample into six subsamples based on their IR detection status and LyC leakage strength (strong, weak, or non-leakers). Our findings include:

1. IR-undetected strong leakers show significantly high O32, consistent with ionization states in density-bound systems. On the other hand, IR-detected strong leakers exhibit O32 similar to weak or non-leakers.
2. IR-undetected strong leakers are characterized by the bluest β_{1200} slopes, the lowest stellar masses, and the lowest dust extinction ($E(B - V)$) among all subsamples. In contrast, IR-detected strong leakers possess significantly higher stellar masses and redder β_{1200} slopes, with O32 and β_{1200} values comparable to those of weak or non-leakers. Despite their high IR luminosities, these IR-detected systems show significantly lower $E(B - V)$ values than the weak and non-leaking populations, indicating that the optical and IR components in these systems likely arise from different sites.
3. The IR-detected strong leakers seem to be more extended than IR-undetected galaxies. According to HST images at optical wavelengths, we find the IR-detected strong leakers tend to be in merger systems, while the IR-undetected strong leakers are more compact.

Incorporating the evidence from the Ly α profiles and radio data, we suggest that the 8 IR-detected strong leakers are more likely leaking LyC photons through clean channels in a porous ISM, whereas the 12 IR-undetected strong leakers show properties consistent with predominantly density-bound conditions.

Recent studies at high redshift, such as [Zhu et al. \(2025\)](#), suggest that LyC leakers are predominantly mergers (20 out of 23 LCEs in GOODS-S sample) but also include a population of compact, extreme starbursts (e.g., [Marques-Chaves et al. 2021, 2024](#); [Kerutt et al.](#)

¹ These observations are made from Proposal ID 14656, 15445, 16427, 14466, and 16245. For some of these images, we remove the cosmic rays using the method described by [van Dokkum \(2001\)](#), with the Python package `astrocrappy` ([McCully & others 2018](#)).

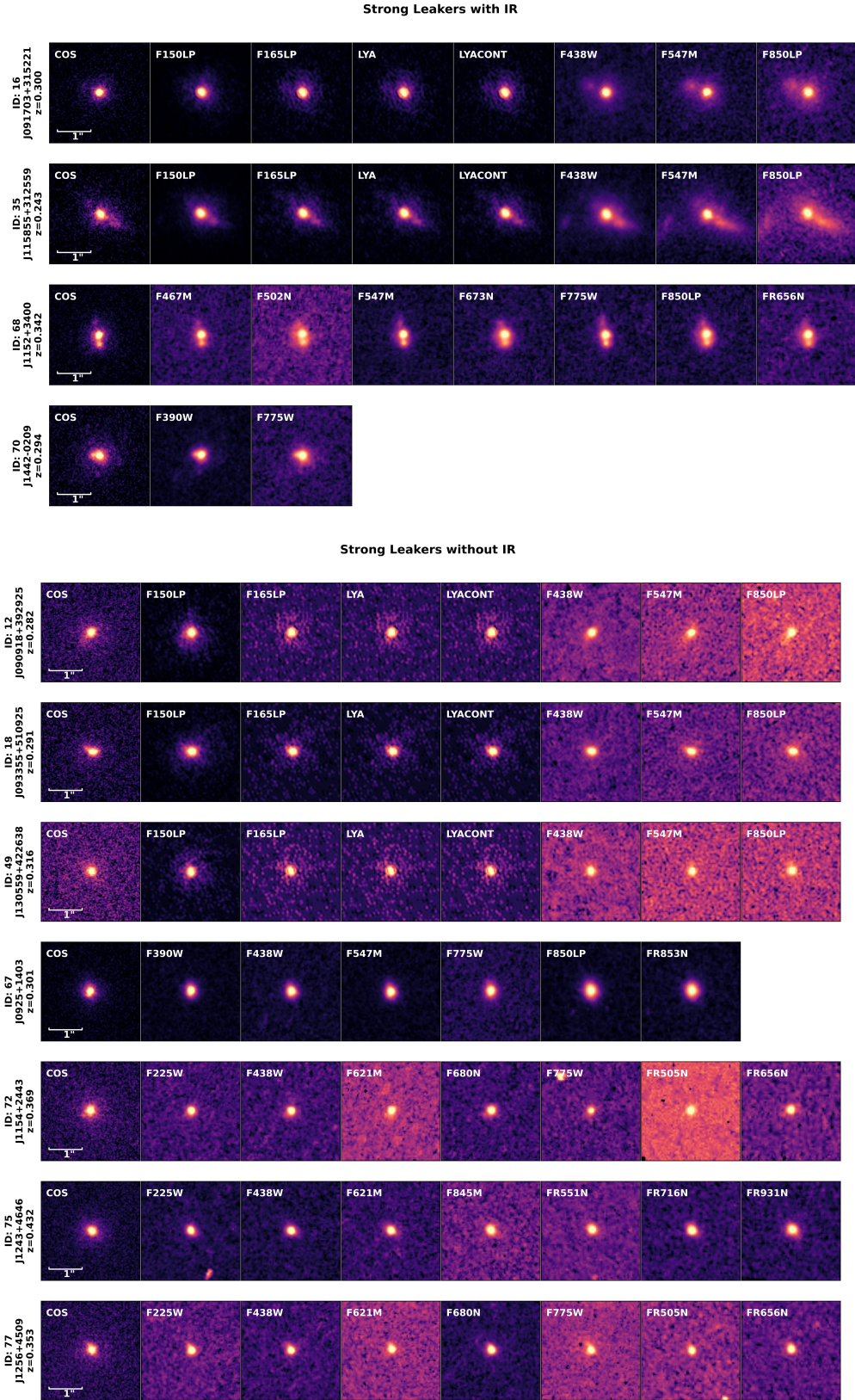


Figure 3. HST images for strong LyC leakers ($f_{\text{esc}} > 5\%$). Top: IR-detected strong leakers. Bottom: IR-undetected strong leakers.

2024; Zhu et al. 2024), pointing toward two distinct escape mechanisms. By categorizing leakers into IR-detected and IR-undetected populations, we identify two groups that naturally exhibit distinct O32 and physical properties. These populations likely represent the theoretical pathways of ionization-bound and density-bound escape, which may correspond to the merger-driven and compact starburst modes, respectively.

In the local sample, IR-undetected strong leakers dominate the total ionizing budget, contributing roughly 67% of the emitted LyC photons, while IR-detected strong leakers provide a smaller but non-negligible fraction ($\sim 20\%$). Given the complex selection function of the sample, these fractions should be interpreted with caution. The substantial dust reservoirs in our IR-detected leakers ($M_{\text{dust}} \approx 1.7 \times 10^7 M_{\odot}$) are comparable to those inferred for dusty EoR galaxies (e.g., Watson et al. 2015; Fudamoto et al. 2021), suggesting that IR-detected strong leakers may be more representative of the dominant reionization sources in a dustier-than-expected early universe (e.g., Sun et al. 2025).

This work is limited by the small sample size and a potential selection bias toward extreme star-forming systems, which may not capture the full diversity of LCEs. Furthermore, the sensitivity and resolution of WISE data restrict our investigation of the IR-faint population; Spitzer archival data, available for only 6 galaxies, provide no additional constraints. Future surveys with larger, more representative samples and improved sensitivity will be essential for quantifying the relative importance of these different escape pathways.

This work is supported by the China Survey Space Telescope (CSST) project dedicated scientific research funds under grant Nos. CMS-CSST-2025-A06, CMS-CSST-2025-A10, CMS-CSST-2025-A17, and CMS-CSST-2025-A18. ZYZ acknowledges the supports by the Shanghai Leading Talent Program of Eastern Talent Plan (LJ2025051) and the China-Chile Joint Research Fund (CCJRF No. 1906).

The *WISE* data used in this work are available from the Infrared Science Archive (IRSA) at IPAC: [10.26131/IRSA1](https://irsa.ipac.caltech.edu/data/IRSA/). The *HST* data can be accessed via MAST: [10.17909/5neh-6959](https://mast.stsci.edu/#/search/10.17909/5neh-6959). This research is based on observations made with the NASA/ESA Hubble Space Telescope obtained from the Space Telescope Science Institute, which is operated by the Association of Universities for Research in Astronomy, Inc., under NASA contract NAS 5-26555. These observations are associated with program(s) 11107, 14131, 14466, 14656, 15445, 16245, 16427, and 17069 (HST imaging), and 13744, 14635, and 15639 (COS spectra).

Funding for the Sloan Digital Sky Survey IV has been provided by the Alfred P. Sloan Foundation, the U.S. Department of Energy Office of Science, and the Participating Institutions. SDSS-IV acknowledges support and resources from the Center for High-Performance Computing at the University of Utah. The SDSS web site is www.sdss.org.

SDSS-IV is managed by the Astrophysical Research Consortium for the Participating Institutions of the SDSS Collaboration including the Brazilian Participation Group, the Carnegie Institution for Science, Carnegie Mellon University, the Chilean Participation Group, the French Participation Group, Harvard-Smithsonian Center for Astrophysics, Instituto de Astrofísica de Canarias, The Johns Hopkins University, Kavli Institute for the Physics and Mathematics of the Universe (IPMU) / University of Tokyo, the Korean Participation Group, Lawrence Berkeley National Laboratory, Leibniz Institut für Astrophysik Potsdam (AIP), Max-Planck-Institut für Astronomie (MPIA Heidelberg), Max-Planck-Institut für Astrophysik (MPA Garching), Max-Planck-Institut für Extraterrestrische Physik (MPE), National Astronomical Observatories of China, New Mexico State University, New York University, University of Notre Dame, Observatório Nacional / MCTI, The Ohio State University, Pennsylvania State University, Shanghai Astronomical Observatory, United Kingdom Participation Group, Universidad Nacional Autónoma de México, University of Arizona, University of Colorado Boulder, University of Oxford, University of Portsmouth, University of Utah, University of Virginia, University of Washington, University of Wisconsin, Vanderbilt University, and Yale University.

REFERENCES

- Álvarez-Márquez, J., Crespo Gómez, A., Colina, L., et al. 2023, *A&A*, 671, A105, doi: [10.1051/0004-6361/202245400](https://doi.org/10.1051/0004-6361/202245400)
- Bait, O., Borthakur, S., Schaerer, D., et al. 2024, *A&A*, 688, A198, doi: [10.1051/0004-6361/202348416](https://doi.org/10.1051/0004-6361/202348416)
- Bergvall, N., Zackrisson, E., Andersson, B.-G., et al. 2006, *A&A*, 448, 513, doi: [10.1051/0004-6361:20053788](https://doi.org/10.1051/0004-6361:20053788)
- Boquien, M., Burgarella, D., Roehly, Y., et al. 2019, *A&A*, 622, A103, doi: [10.1051/0004-6361/201834156](https://doi.org/10.1051/0004-6361/201834156)
- Borthakur, S., Heckman, T. M., Leitherer, C., & Overzier, R. A. 2014, *Science*, 346, 216, doi: [10.1126/science.1254214](https://doi.org/10.1126/science.1254214)
- Burgarella, D., Buat, V., & Iglesias-Páramo, J. 2005, *MNRAS*, 360, 1413, doi: [10.1111/j.1365-2966.2005.09131.x](https://doi.org/10.1111/j.1365-2966.2005.09131.x)
- Burgarella, D., Nanni, A., Hirashita, H., et al. 2020, *A&A*, 637, A32, doi: [10.1051/0004-6361/201937143](https://doi.org/10.1051/0004-6361/201937143)
- Cardelli, J. A., Clayton, G. C., & Mathis, J. S. 1989, *ApJ*, 345, 245, doi: [10.1086/167900](https://doi.org/10.1086/167900)
- Chisholm, J., Saldana-Lopez, A., Flury, S., et al. 2022, *MNRAS*, 517, 5104, doi: [10.1093/mnras/stac2874](https://doi.org/10.1093/mnras/stac2874)
- Cormier, D., Lebouteiller, V., Madden, S. C., et al. 2012, *A&A*, 548, A20, doi: [10.1051/0004-6361/201219818](https://doi.org/10.1051/0004-6361/201219818)
- Cutri, R. M., Wright, E. L., Conrow, T., et al. 2013, Explanatory Supplement to the AllWISE Data Release Products, Explanatory Supplement to the AllWISE Data Release Products, by R. M. Cutri et al.
- de Barros, S., Vanzella, E., Amorín, R., et al. 2016, *A&A*, 585, A51, doi: [10.1051/0004-6361/201527046](https://doi.org/10.1051/0004-6361/201527046)
- Deharveng, J.-M., Buat, V., Le Brun, V., et al. 2001, *A&A*, 375, 805, doi: [10.1051/0004-6361:20010920](https://doi.org/10.1051/0004-6361:20010920)
- Draine, B. T., Aniano, G., Krause, O., et al. 2014, *ApJ*, 780, 172, doi: [10.1088/0004-637X/780/2/172](https://doi.org/10.1088/0004-637X/780/2/172)
- Flury, S. R., Jaskot, A. E., Ferguson, H. C., et al. 2022a, *ApJS*, 260, 1, doi: [10.3847/1538-4365/ac5331](https://doi.org/10.3847/1538-4365/ac5331)
- . 2022b, *ApJ*, 930, 126, doi: [10.3847/1538-4357/ac61e4](https://doi.org/10.3847/1538-4357/ac61e4)
- Fudamoto, Y., Oesch, P. A., Schouws, S., et al. 2021, *Nature*, 597, 489, doi: [10.1038/s41586-021-03846-z](https://doi.org/10.1038/s41586-021-03846-z)
- Grimes, J. P., Heckman, T., Aloisi, A., et al. 2009, *ApJS*, 181, 272, doi: [10.1088/0067-0049/181/1/272](https://doi.org/10.1088/0067-0049/181/1/272)
- Gupta, A., Trott, C. M., Jaiswar, R., et al. 2024, arXiv e-prints, arXiv:2403.13285, doi: [10.48550/arXiv.2403.13285](https://doi.org/10.48550/arXiv.2403.13285)
- Heckman, T. M., Sembach, K. R., Meurer, G. R., et al. 2001, *ApJ*, 558, 56, doi: [10.1086/322475](https://doi.org/10.1086/322475)
- Heckman, T. M., Borthakur, S., Overzier, R., et al. 2011, *ApJ*, 730, 5, doi: [10.1088/0004-637X/730/1/5](https://doi.org/10.1088/0004-637X/730/1/5)
- Hu, W., Martin, C. L., Gronke, M., et al. 2023, *ApJ*, 956, 39, doi: [10.3847/1538-4357/aceefd](https://doi.org/10.3847/1538-4357/aceefd)
- Izotov, Y. I., Orlitová, I., Schaerer, D., et al. 2016a, *Nature*, 529, 178, doi: [10.1038/nature16456](https://doi.org/10.1038/nature16456)
- Izotov, Y. I., Schaerer, D., Thuan, T. X., et al. 2016b, *MNRAS*, 461, 3683, doi: [10.1093/mnras/stw1205](https://doi.org/10.1093/mnras/stw1205)
- Izotov, Y. I., Schaerer, D., Worseck, G., et al. 2018a, *MNRAS*, 474, 4514, doi: [10.1093/mnras/stx3115](https://doi.org/10.1093/mnras/stx3115)
- Izotov, Y. I., Worseck, G., Schaerer, D., et al. 2018b, *MNRAS*, 478, 4851, doi: [10.1093/mnras/sty1378](https://doi.org/10.1093/mnras/sty1378)
- Jaskot, A. E., Silveyra, A. C., Plantinga, A., et al. 2024, *ApJ*, 972, 92, doi: [10.3847/1538-4357/ad58b9](https://doi.org/10.3847/1538-4357/ad58b9)
- Ji, Z., Alberts, S., Zhu, Y., et al. 2025, *ApJL*, 988, L69, doi: [10.3847/2041-8213/adf194](https://doi.org/10.3847/2041-8213/adf194)
- Kakiichi, K., & Gronke, M. 2021, *ApJ*, 908, 30, doi: [10.3847/1538-4357/abc2d9](https://doi.org/10.3847/1538-4357/abc2d9)
- Kerutt, J., Oesch, P. A., Wisotzki, L., et al. 2024, *A&A*, 684, A42, doi: [10.1051/0004-6361/202346656](https://doi.org/10.1051/0004-6361/202346656)
- Laporte, N., Ellis, R. S., Boone, F., et al. 2017, *ApJL*, 837, L21, doi: [10.3847/2041-8213/aa62aa](https://doi.org/10.3847/2041-8213/aa62aa)
- Le Reste, A., Jaskot, A. E., Brazie, J., et al. 2025, arXiv e-prints, arXiv:2509.06922, doi: [10.48550/arXiv.2509.06922](https://doi.org/10.48550/arXiv.2509.06922)
- Le Reste, Alexandra. 2025, Source data for LaCOS (LeReste+2025), STScI/MAST, doi: [10.17909/5NEH-6959](https://doi.org/10.17909/5NEH-6959)
- Leitet, E., Bergvall, N., Hayes, M., Linné, S., & Zackrisson, E. 2013, *A&A*, 553, A106, doi: [10.1051/0004-6361/201118370](https://doi.org/10.1051/0004-6361/201118370)
- Leitherer, C., Ferguson, H. C., Heckman, T. M., & Lowenthal, J. D. 1995, *ApJL*, 454, L19, doi: [10.1086/309760](https://doi.org/10.1086/309760)
- Marques-Chaves, R., Schaerer, D., Álvarez-Márquez, J., et al. 2021, *MNRAS*, 507, 524, doi: [10.1093/mnras/stab2187](https://doi.org/10.1093/mnras/stab2187)
- Marques-Chaves, R., Schaerer, D., Vanzella, E., et al. 2024, *A&A*, 691, A87, doi: [10.1051/0004-6361/202451667](https://doi.org/10.1051/0004-6361/202451667)
- Mascia, S., Pentericci, L., Llerena, M., et al. 2025, *A&A*, 701, A122, doi: [10.1051/0004-6361/202553760](https://doi.org/10.1051/0004-6361/202553760)
- Maulick, S., & Saha, K. 2026, arXiv e-prints, arXiv:2601.17746, doi: [10.48550/arXiv.2601.17746](https://doi.org/10.48550/arXiv.2601.17746)
- Maulick, S., Saha, K., & Rutkowski, M. J. 2025, *ApJ*, 984, 40, doi: [10.3847/1538-4357/adc10e](https://doi.org/10.3847/1538-4357/adc10e)
- McCully, C., & others. 2018, astrocrappy: Speed-optimized L.A.Cosmic, <https://doi.org/10.5281/zenodo.1482018>, Zenodo, doi: [10.5281/zenodo.1482018](https://doi.org/10.5281/zenodo.1482018)
- Nakajima, K., Ellis, R. S., Robertson, B. E., Tang, M., & Stark, D. P. 2020, *ApJ*, 889, 161, doi: [10.3847/1538-4357/ab6604](https://doi.org/10.3847/1538-4357/ab6604)
- Noll, S., Burgarella, D., Giovannoli, E., et al. 2009, *A&A*, 507, 1793, doi: [10.1051/0004-6361/200912497](https://doi.org/10.1051/0004-6361/200912497)

- Overzier, R. A., Heckman, T. M., Tremonti, C., et al. 2009, *ApJ*, 706, 203, doi: [10.1088/0004-637X/706/1/203](https://doi.org/10.1088/0004-637X/706/1/203)
- Pahl, A., Shapley, A., Steidel, C. C., et al. 2024, *ApJ*, 974, 212, doi: [10.3847/1538-4357/ad725d](https://doi.org/10.3847/1538-4357/ad725d)
- Pahl, A. J., Shapley, A., Steidel, C. C., et al. 2023, *MNRAS*, 521, 3247, doi: [10.1093/mnras/stad774](https://doi.org/10.1093/mnras/stad774)
- Rivera-Thorsen, T. E., Le Reste, A., Hayes, M. J., et al. 2025, arXiv e-prints, arXiv:2512.19967, doi: [10.48550/arXiv.2512.19967](https://doi.org/10.48550/arXiv.2512.19967)
- Roy, N., Heckman, T., Henry, A., et al. 2025, *ApJ*, 992, 91, doi: [10.3847/1538-4357/adff5e](https://doi.org/10.3847/1538-4357/adff5e)
- Saha, K., Tandon, S. N., Simmonds, C., et al. 2020, *Nature Astronomy*, 4, 1185, doi: [10.1038/s41550-020-1173-5](https://doi.org/10.1038/s41550-020-1173-5)
- Saldana-Lopez, A., Schaerer, D., Chisholm, J., et al. 2022, *A&A*, 663, A59, doi: [10.1051/0004-6361/202141864](https://doi.org/10.1051/0004-6361/202141864)
- Schaerer, D., Hayes, M., Verhamme, A., & Teyssier, R. 2011, *A&A*, 531, A12, doi: [10.1051/0004-6361/201116709](https://doi.org/10.1051/0004-6361/201116709)
- Stern, D., Assef, R. J., Benford, D. J., et al. 2012, *ApJ*, 753, 30, doi: [10.1088/0004-637X/753/1/30](https://doi.org/10.1088/0004-637X/753/1/30)
- Sun, F., Yang, J., Wang, F., et al. 2025, arXiv e-prints, arXiv:2506.06418, doi: [10.48550/arXiv.2506.06418](https://doi.org/10.48550/arXiv.2506.06418)
- van Dokkum, P. G. 2001, *Publications of the Astronomical Society of the Pacific*, 113, 1420, doi: [10.1086/323894](https://doi.org/10.1086/323894)
- Vanzella, E., de Barros, S., Vasei, K., et al. 2016, *ApJ*, 825, 41, doi: [10.3847/0004-637X/825/1/41](https://doi.org/10.3847/0004-637X/825/1/41)
- Verhamme, A., Orlitová, I., Schaerer, D., & Hayes, M. 2015, *A&A*, 578, A7, doi: [10.1051/0004-6361/201423978](https://doi.org/10.1051/0004-6361/201423978)
- Wang, B., Heckman, T. M., Leitherer, C., et al. 2019, *ApJ*, 885, 57, doi: [10.3847/1538-4357/ab418f](https://doi.org/10.3847/1538-4357/ab418f)
- Wang, S., Wang, X., Malkan, M. A., et al. 2025, arXiv e-prints, arXiv:2512.23202, doi: [10.48550/arXiv.2512.23202](https://doi.org/10.48550/arXiv.2512.23202)
- Watson, D., Christensen, L., Knudsen, K. K., et al. 2015, *Nature*, 519, 327, doi: [10.1038/nature14164](https://doi.org/10.1038/nature14164)
- Wright, E. L., Eisenhardt, P. R. M., Mainzer, A. K., & et al. 2019, *AllWISE Source Catalog, IPAC/IRSA*, doi: [10.26131/IRSA1](https://doi.org/10.26131/IRSA1)
- Wright, E. L., Eisenhardt, P. R. M., Mainzer, A. K., et al. 2010, *AJ*, 140, 1868, doi: [10.1088/0004-6256/140/6/1868](https://doi.org/10.1088/0004-6256/140/6/1868)
- Yuan, F.-T., Zheng, Z.-Y., Jiang, C., et al. 2024, *ApJ*, 975, 53, doi: [10.3847/1538-4357/ad75ff](https://doi.org/10.3847/1538-4357/ad75ff)
- Yuan, F.-T., Zheng, Z.-Y., Lin, R., Zhu, S., & Rahna, P. T. 2021, *ApJL*, 923, L28, doi: [10.3847/2041-8213/ac4170](https://doi.org/10.3847/2041-8213/ac4170)
- Zhu, S., Yuan, F.-T., Jiang, C., Zheng, Z.-Y., & Lin, R. 2024, *ApJL*, 974, L20, doi: [10.3847/2041-8213/ad7b18](https://doi.org/10.3847/2041-8213/ad7b18)
- Zhu, S., Zheng, Z.-Y., Yuan, F.-T., Jiang, C., & Lin, R. 2025, *ApJL*, 982, L58, doi: [10.3847/2041-8213/adc125](https://doi.org/10.3847/2041-8213/adc125)